



HAL
open science

Instrumented indentation on alumina-alumina/zirconia multilayered composites with residual stresses

Emilio Jiménez-Piqué, Luca Ceseracciu, Yves Gaillard, Mylene Brach,
Goffredo de Portu, Marc Anglada

► **To cite this version:**

Emilio Jiménez-Piqué, Luca Ceseracciu, Yves Gaillard, Mylene Brach, Goffredo de Portu, et al.. Instrumented indentation on alumina-alumina/zirconia multilayered composites with residual stresses. *Philosophical Magazine*, 2006, 86 (33-35), pp.5371-5382. 10.1080/14786430600681621 . hal-00513690

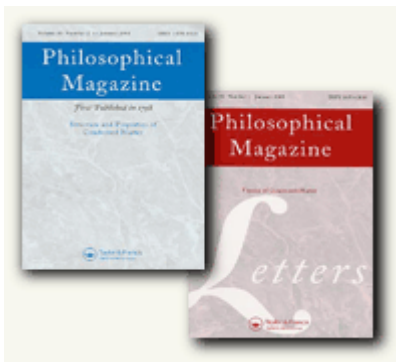
HAL Id: hal-00513690

<https://hal.science/hal-00513690>

Submitted on 1 Sep 2010

HAL is a multi-disciplinary open access archive for the deposit and dissemination of scientific research documents, whether they are published or not. The documents may come from teaching and research institutions in France or abroad, or from public or private research centers.

L'archive ouverte pluridisciplinaire **HAL**, est destinée au dépôt et à la diffusion de documents scientifiques de niveau recherche, publiés ou non, émanant des établissements d'enseignement et de recherche français ou étrangers, des laboratoires publics ou privés.



Instrumented indentation on alumina-alumina/zirconia multilayered composites with residual stresses

Journal:	<i>Philosophical Magazine & Philosophical Magazine Letters</i>
Manuscript ID:	TPHM-05-Nov-0526.R2
Journal Selection:	Philosophical Magazine
Date Submitted by the Author:	09-Feb-2006
Complete List of Authors:	Jiménez-piqué, Emilio; UPC, CMEM ceseracciu, Luca; UPC, CMEM gaillard, yves; UPC, CMEM Brach, Mylene; National Research Council, Institute of Science and Technology for Ceramics de Portu, Goffredo; National Research Council, Institute of Science and Technology for Ceramics anglada, marc; UPC, CMEM
Keywords:	residual stress, alumina, brittle materials, ceramics, contact mechanics, indentation, multilayers, nanoindentation
Keywords (user supplied):	



Instrumented indentation on alumina-alumina/zirconia multilayered composites with residual stresses

E. Jiménez-Piqué^{1*}, L. Ceseracciu¹, Y. Gaillard¹, M. Barch², G. de Portu², M. Anglada¹

¹Departamento de Ciencia de Materiales e Ingeniería Metalúrgica. Universitat Politècnica de Catalunya. Avda. Diagonal 647 (ETSEIB) 08028 Barcelona, SPAIN

²National Research Council (CNR). Institute of Science and Technology for Ceramics (ISTEC). 48018 Faenza (RA), Italy.

*Corresponding author: emilio.jimenez@upc.es Tel: +34 934054454, FAX: +34 934016706

In this work the instrumented indentation response of polycrystalline alumina and alumina-based ceramic multilayers with well known residual stresses have been investigated. Young's modulus and hardness were evaluated as a function of penetration depth with Berkovich and spherical indenters by continuous stiffness measurements. A size effect was observed due to the length scale of the microstructure. Values of hardness and Young's modulus obtained were in good agreement with previous works. No significant differences in the P-h curves were observed for materials with and without residual stress, making, then, difficult to employ the different methodologies derived for estimation of residual stress or crack length evaluation existing in the literature. Crack length had therefore to be measured by direct observation. In this respect, cube corner indentations did not produce well-developed radial cracks but chipping of the material, whereas indentations with Berkovich indenters produce radial cracks suitable for apparent fracture toughness estimation, and, consequently, residual stress.

1 Introduction

Recently, ceramic multilayered composites have received much attention due to their superior mechanical properties and reliability compared to monolithic ceramics [1, 2, 3]. This increase in mechanical properties in multilayers can be achieved through different strategies such as weak interfaces [4], containment of martensitic transformation [5], existence of porous layers [6] or introduction of compressive stresses [7,8]. This latter approach is one of the most usual ones, and it is normally achieved by stacking alternating layers of materials with different thermal expansion coefficients that will translate in residual stresses during cooling in the sintering stage.

Among the ceramic multilayered composites that can be produced, one of the most preferred material combinations is alumina and zirconia. Usually, at least one of the layers of the composite is made of an alumina/zirconia composite, in order to tailor the coefficient of thermal expansion (CTE) and, consequently, the residual stresses. In this way, the channel cracking produced during sintering can be avoided. The reason for choosing alumina and zirconia as the constituent materials of ceramic laminates is generally because of the excellent bonding between the layers in the absence of excessive diffusion between components, their good thermo-mechanical properties and their relatively ease of processing. In addition, alumina layers are generally placed on

Deleted: than

1
2 the surface, because are the ones to have compressive residual stresses and higher
3 hardness (H).
4

5 These ceramic multilayers have shown improved fracture toughness [9], reliability [10],
6 wear behaviour [11] and contact resistance [12, 13] than their monolithic counterparts,
7 due, principally, to their residual stress. Correct assessment of this residual stress is,
8 therefore, a key factor in these materials. Calculation of the residual stress can be done
9 by modelling the different shrinkage behaviour of the layers and observed by different
10 spectroscopic techniques, such as micro-Raman [14] or X-ray diffraction. However,
11 during utilization in thermo-mechanical demanding applications, the surface will be
12 damaged in different ways (such as microcracking, deformation, wear, ...) that can alter
13 the local distribution of residual stresses. These residual stresses should be correctly
14 evaluated in order to estimate the life time of the component.
15

16 Instrumented indentation is, a priori, a good technique for local evaluation of the
17 residual stresses, and, for that purpose, several methods have been developed, specially
18 for metals with relatively low yield stress and that do not work harden appreciably when
19 indented with sharp indenters. Most of these methods are based in the change in contact
20 areas with and without residual stress, such as in the works of Suresh and
21 Giannakopoulos [15], Tsui et al [16] or the change in the elastic penetration depth, as
22 the work of Xu and Li [17]. Swadener et al. [18] used spherical indenters instead of
23 sharp indenters, and showed that blunt indentation is more sensitive to residual stress
24 than sharp indentation.
25

Deleted: stress and that the estimation of residual stress can be estimated with more precision.

26 However, for the case of hard and brittle materials the residual stress is normally
27 estimated by indentation fracture methods, which imply that the crack length produced
28 by a sharp probe has to be visualized [19]. In this case, the use of a cube-corner indenter
29 instead of a Berkovich indenter is preferred, because the fracture threshold can be
30 lowered several orders of magnitude [20, 21]. Recently several methods for fracture
31 toughness estimation without visualization of the crack length have been proposed, for
32 example the works of Field et al. [22], where they relate the crack length produced to
33 the pop-in behaviour during loading or the work of Dahami et al. [23] where they
34 related the crack length with the total penetration depth for fused silica.
35

36 Despite the fact that alumina is a relatively widespread technical ceramic, there are only
37 few studies on indentation on polycrystalline alumina. In one of the first systematic
38 studies, Krell and Schädlich [24] reported a size effect on the hardness measurement.
39 Recently, Gong et al [25] studied the effect of the microstructural inhomogeneity on the
40 reproducibility of data in fine-grained alumina, observing a size effect on hardness and a
41 large scatter of values on both hardness and Young's modulus (E), specially when the
42 indentation dimensions were comparable to the characteristic microstructural
43 dimensions. Similar trends were observed in studies using Vickers indenters by Ullner
44 and co-workers [26], and using cube-corner indenters by Twigg et al. [27], though
45 without reporting values of hardness for different loads. In this last case a certain
46 amount of pop in was observed which was attributed to radial cracking, though not
47 direct proof of this was given. In all previous studies in polycrystalline alumina it has
48 always been observed a higher Young modulus than the one for bulk materials (380 –
49 400 GPa) and a strong size effect. There are also few data on the continuous value of E ,
50 H as a function of penetration depth, although there are some attempts to obtain such a
51 relationship by analysis of the loading curve [24].
52
53
54
55
56
57
58
59
60

Deleted: and a large scatter of values

1
2
3
4
5
6
7
8
9
10
11
12
13
14
15
16
17
18
19
20
21
22
23
24
25
26
27
28
29
30
31
32
33
34
35
36
37
38
39
40
41
42
43
44
45
46
47
48
49
50
51
52
53
54
55
56
57
58
59
60

The objective of this work is then twofold: first, to analyze the values of E , H as a function of the indentation depth for both Berkovich and spherical indenters on alumina and, second, to compare different methods for evaluation of the residual stress in alumina-alumina/zirconia laminated composites.

2 Experimental

2.1 Material preparation

To obtain the ceramic sheets suitable for the preparation of laminated composites, two powders were used: high purity (99.7%) alumina (Alcoa A16 -SG, Alcoa Aluminium Co., New York, USA) with an average particle size of 0.3 μm , and tetragonal zirconia polycrystals (TZ3Y-S, Tosho Corp. Japan) containing 94.7 % of ZrO_2 and 3 mol% of Y_2O_3 (usually referred to as 3Y-TZP) with an average particle size of 0.3 μm .

The different powders were mixed with organic binders, dispersant, plasticizers and solvents to obtain suitable slips for tape casting. After mixing with organic components, the slurry containing the ceramic powders was tape casted onto a mylar sheet moved at a constant speed of 200 mm/min. Details on this technique can be found elsewhere [28].

Sheets of pure alumina as well as of the composite alumina-zirconia in the volume ratio 60/40 were prepared. The thickness of the green tapes were selected in order to obtain, after sintering, layers of about 200 μm (alumina) and 250 μm (alumina-zirconia). After drying, laminae of 50 x 34 mm were cut from the different ceramic sheets. Hybrid laminates were prepared by stacking and warm pressing the green sheets at 75 $^\circ\text{C}$ at a pressure of 30 MPa for 30 minutes. Different samples were obtained by alternately superimposing one layer of alumina and one layer of alumina-zirconia (this structure is hereinafter designated A/AZ) or one layer of alumina and two layer of alumina-zirconia (hereinafter designated A/2AZ). The structures were designed in order to have always an alumina layer in both outer surfaces. Debonding was carried out with a very slow heating rate up to 600 $^\circ\text{C}$, followed by sintering at 1550 $^\circ\text{C}$ for 1 h. We thus obtained dense samples (97% of theoretical density) with a thickness of about 3.0 mm, containing layers with a thickness ratio of about 1/1.3 (A/AZ) and 1/2.6 (A/2AZ). In the hybrid samples, due to lower thermal expansion coefficient and shrinkage during sintering, the external alumina layers undergo residual compressive stresses. As reference material (i.e. nominally stress free), pure monolithic alumina (A) was prepared by cold isostatic pressing and sintering at 1550 $^\circ\text{C}$ for 1 h. A view of the samples obtained and the interface is presented in figure 1 (a) and (b), respectively.

Residual stresses on A/AZ composites were estimated by different methods: a) finite element analysis gives a value of 240 MPa; b) fluorescence measurements on these materials give values of about 150 MPa [29]; c) comparison of apparent fracture toughness by Vickers indentation [12] gives a value of 180 MPa.

Samples were cut into prismatic samples of 5 by 10 mm and lightly polished with diamond suspension up to 3 μm with a low applied force in order to avoid excessive loss of material, with a final polishing of colloidal silica.

2.2 Instrumented indentation

Instrumented indentation tests were performed in a fully calibrated MTS Nanoindenter XP (Nanoinstruments Innovation Center, MTS systems, TN, USA) equipped with CSM (continuous stiffness measurement). Three diamond indenters, Berkovich, spherical (25 μm radius) and cube-corner were used. Indentations were done in the top alumina layer of the A/AZ multilayered composites far from the edge in order to assure a constant residual stress for all three indenter types and in A/2AZ with the Berkovich indenter. Some tests were also done in the lateral face of the sample in the middle of alumina layers. Figure 1(c) presents schematically the location of the different indentation places. At least nine indentations were done for each condition and the results were averaged.

Results obtained with the Berkovich indenter were analysed with the well-known Oliver and Pharr method [30]. However, the factor β (which takes into account the lateral displacements and the non-axisymmetry of the indenter) in the expression of the relationship between reduced Young's modulus E_r and stiffness (S) was not taken constant but dependant on the Poisson ratio, ν , as suggested in the works of Pharr and co-workers [31, 32]:

$$S = \beta(\nu) \frac{2}{\sqrt{\pi}} E_r \sqrt{A} \quad (1)$$

where A is the contact area and $\beta(\nu)$ is taken after Hay et al [32]. Poisson ratio for alumina was taken equal to 0.26.

In the case of the spherical indenter, the Young modulus was calculated using the classical Hertzian formulation [33,34]. Hardness values were not calculated because it will require the determination of the true curvilinear shape of the surface under the indenter. For the cube corner no calculation of E , H was made because of the relative large amount of friction [35].

Indentation imprints were visualized with scanning electron and atomic force microscopy (Veeco Multimode).

3 Results and discussion

3.1 Extraction of mechanical properties

a) Berkovich indenter

Figure 2 presents the load (P) vs. penetration depth (h) in the monolithic alumina (A) and in the two multilayered composites (A/AZ and A/2AZ) indented on the top layer. Figure 3 presents the values of E and H as a function of the penetration depth obtained with the CSM technique.

1
2
3
4
5
6
7
8
9
10
11
12
13
14
15
16
17
18
19
20
21
22
23
24
25
26
27
28
29
30
31
32
33
34
35
36
37
38
39
40
41
42
43
44
45
46
47
48
49
50
51
52
53
54
55
56
57
58
59
60

It is seen that there is no appreciable differences in the P - h curves of the three different materials, despite the different residual stresses, neither in the loading portion nor in the unloading portion of the indentation cycle. Therefore, it is not feasible to apply any of the existing methodologies [15, 16, 17, 23] to extract values of residual stress. This result was already expected because of two main reasons: first, compressive residual stresses do not produce a large change in the P - h curves [16], and, second because of the high hardness and, consequently, yield stress of alumina in relation with the residual stress. A simple modelling by finite element analysis was performed using an axisymmetric indenter on a purely elastic solid with the material properties and residual stresses of these materials, with boundary conditions such that there is no border effect on the elastic field (model radial dimension > 50 times the contact radius, thickness same as the actual samples). The simulation showed that the effect of residual stresses on penetration depths is of only about 0.3%. This difference is well below the scatter experimentally observed.

Field Code Changed

Deleted: shows

Deleted:

Inspection of the residual imprints by atomic force microscopy does not yield a difference in the residual contact areas of materials A and A/AZ. In both cases both materials clearly show sink-in, validating in part the methodology for extraction of mechanical properties, and comparable contact areas, of around $9.5 \mu\text{m}^2$ for a penetration depth of $1 \mu\text{m}$. Figure 4 presents AFM images of Berkovich indentations with $1 \mu\text{m}$ maximum penetration depth ($P \approx 450\text{mN}$) on A and A/AZ.

Regarding the values of E and H obtained by continuous stiffness measurement, it is seen that they are in reasonable agreement with other works. In the case of hardness, we obtained values between 25 to 30 GPa depending on the indentation depth, whereas Gong et al. [25] obtained 20 ± 6 GPa and Krell et al. [24] obtained between 25 and 30 GPa. It is worth noting that using an improved relationship of S and E_r gives values of Young's modulus closer to the values obtained by other methodologies. If, instead of equation 1, the formulation of Oliver & Pharr setting a constant factor β , the value of E will be slightly overestimated, up to 10%.

In both cases, a size effect is observed for all materials, for the hardness readings. This size effect is most probably due to the heterogeneities in the microstructure. Average grain size is $2 \mu\text{m}$, which means that for the maximum penetration depth of $1.2 \mu\text{m}$ the response is given only by a small amount of grains, specially for the H measurements [25].

Deleted: , for both E and H and especially

b) Spherical indenter

In figure 5 the P - h and E - h curves for spherical indentation are presented. Again, it is seen that P - h curves of the stressed and stress-free material are identical from an experimental point of view. Therefore, it is not easy to apply instrumented indentation methodologies for estimation of the residual stress for such hard and stiff materials, although these could be more sensitive to residual stress. This was expected as these methodologies were developed for much softer materials with values of residual stress close to the value of yield stress and the range of residual stresses and material properties considered here are well beyond the original scope of the methodologies. Moreover, the difficulty in setting the correct surface contact point for spherical indentation introduces an extra degree of experimental uncertainty that will mask any possible effects on the response of the material to indentation.

1
2 The value of Young modulus is correctly obtained and matches the values for
3 polycrystalline alumina obtained by other methods. Once more, a size effect for small
4 penetration depths is observed which can be attributed to the microstructural
5 characteristic size.
6
7

8 **3.2 Fracture behaviour**

9

10 a) Cube-corner indenter

11
12 Despite the a priori advantages of cube corner indenters over other type of sharp
13 indenters because of the lower fracture threshold, allowing, therefore, for a more local
14 estimation of residual stress based on fracture mechanics, the indentation in both A and
15 A/AZ materials did not result in well developed radial cracking but in severe chipping.
16 No differences were observed between the stressed and the non-stressed material.
17

18
19 | Chipping was due to the large deformation strain produced by the sharp indenter, and
20 was observed for a wide range of indentation loads, from 100mN up to 10N. The
21 correspondent *P-h* curves of the indentations produced with this indenter presented a
22 severe amount of displacements bursts (pop-in) associated with the processes of
23 formation, growth and spallation during chipping. Figure 6 presents typical curves
24 obtained with cube corner, together with the SEM image of an indentation imprint, were
25 the chipping is clearly appreciated.
26

Deleted: high

Deleted: volume

27 b) Berkovich Indenter

28

29 For sufficiently high loads, radial cracks can be produced with Berkovich indenters (see
30 figure 4). This load is above the fracture threshold level of 200mN [24]. It is seen that
31 the radial crack system appears in the A material. However, in the case of the A/AZ
32 material these cracks are not present. This behaviour may be associated to the
33 compressive residual stress of the laminated materials that decreases the effective stress
34 intensity factor.
35

36 As commented in the introduction, there are several methodologies that have been
37 developed for estimation of the crack length produced during indentation, either by
38 differences in the maximum penetration depth [23] or by the incremental penetration
39 depth produced during pop-in events [22], which can be also related to the different
40 penetration depth of cracked and uncracked material. However, inspection of the *P-h*
41 curves, as said before, reveals no difference between stressed and unstressed material,
42 therefore any crack length estimation will lead to a similar value, which will imply that
43 no value of residual stress could be extracted. Moreover, the possible pop-in observed in
44 the curves may be attributed to other cracking events than radial crack, as, for example
45 chipping.
46

47 In order to estimate the residual stress from changes in apparent fracture toughness, 20
48 indentations were made in the lateral face of the sample, that is, in the middle of an
49 internal sample. The reason for that is that in the lateral location residual stresses
50 perpendicular to the lateral face surface change in sign, from compression to tension,
51 but with the same absolute value [36]. Residual stresses parallel to the interface remain
52
53
54
55
56
57
58
59
60

1
2 equal than in the bulk of the material. In this way, well-developed radial cracks could be
3 produced that fulfilled the conditions for fracture toughness estimations, as is seen in
4 figure 7. In this figure it can also be appreciated the asymmetry of the residual stresses,
5 developing a long crack parallel to the interface but only small cracks in other
6 directions. Spherical indentations also produce cracking, due to the deformation volume
7 underneath the indentation.
8

9 After measurement of 10 crack lengths placed in this location in the A/AZ material and
10 in the A sample, the apparent fracture toughness can be calculated [20], from which the
11 residual stress can be estimated to be: 184 ± 18 MPa. This is in very good agreement
12 with theoretical calculations and measurements done by other methods.
13

14 4 Conclusions

15
16 Extraction of mechanical properties with Berkovich indenters based on the Oliver and
17 Pharr method is satisfactorily done in polycrystalline alumina, although some
18 corrections in the β factor may be advisable for better accuracy in the determination of
19 Young's modulus. This Young modulus is also correctly estimated with spherical
20 indenters using the classical Hertzian theory.
21

22
23 In both E and H measurements there is a strong size effect, which can be attributed to
24 the fact that the microstructural characteristic length, specially the grain size, is
25 comparable to the indentation depth.
26

27 The residual stress did not produce any appreciable change in the $P-h$ curves for any of
28 the laminated materials, making it impossible to use the methodologies based on the
29 influence of the residual stress on the yield stress or the ones that estimate the crack
30 length produced after changes in $P-h$ curves. Therefore it is always necessary to
31 visualize the indentation crack for these materials.
32

Deleted: in

Deleted: s

Deleted: in

33 Cube corner indentations, which may, in principle, produce radial cracking with lower
34 loads, were not adequate for polycrystalline alumina materials, as chipping of the
35 material was the main fracture process instead of well-developed radial cracks.
36 Berkovich indentations induced instead well-developed cracks, which were adequate for
37 calculation of apparent fracture toughness and estimation of the residual stress. It was
38 also seen that the fracture threshold for laminated ceramics with residual stress is higher
39 than the one for stress-free alumina.
40

41 5 Acknowledgements

42 Work supported in part by the European Community's Human Potential Programme
43 under contract HPRN-CT-2002-00203, [SICMAC] and by the Spanish Ministry of
44 Science and Technology, through grant MAT-2002-00368.

45 L.C., Y.G. and M.B. acknowledge the financial support provided through the European
46 Community's Human Potential Programme under contract HPRN-CT-2002-00203,
47 [SICMAC].
48
49
50
51
52
53
54
55
56
57
58
59
60

6 Bibliography

- 1 [1] J.S. Moya, Adv. Mater. **7** 185 (1995)
- 2 [2] H. M. Chan, Annu. Rev. Mater. Sci. **27** 249 (1997)
- 3 [3] M.P. Harner, H.M. Chan and G. A. Miller, J. Am. Ceram. Soc. **75** 1715 (1992)
- 4 [4] J.R. Mawdsley, D. Kovar and J.W. Halloran, J. Am. Ceram. Soc. **83** 802 (2000)
- 5 [5] D.B. Marshall, J.J. Ratto and F. F. Lange, J. Am. Ceram. Soc. **74** 2979 (1991)
- 6 [6] B. F. Sorensen and A. Horsewell, J. Am. Ceram. Soc. **84** 2051 (2001)
- 7 [7] J. Requena, R. Moreno and J. S. Moya, J. Am. Ceram. Soc. **72** 1511(1989)
- 8 [8] K.C Goretta, F. Gutiérrez-Mora, J.J. Picciolo and J.L. Routbort, Mat. Sci. Eng. A
- 9 **341** 158 (2003)
- 10 [9] R. J. Moon, K.J. Bowman, K. P. Trumble and J. Rödel, Acta Mater **49** 995 (2001)
- 11 [10] A.J. Sánchez-Herencia, C. Pascual, J. He and F.F.Lange, J. Am. Ceram. Soc. **82**
- 12 1512 (1999)
- 13 [11] F. Toschi, C. Melandri, P. Pinasco, E. Roncari, S. Guicciardi and G. de Portu, J.
- 14 Am. Ceram. Soc. **86** 1547 (2003)
- 15 [12] E.Jiménez-Piqué, L. Ceseracciu, F. Chalvet, M. Anglada and G. de Portu, J. Eur.
- 16 Ceram. Soc. **25** 3393 (2005)
- 17 [13] L. Ceseracciu, F. Chalvet, , G. de Portu, M. Anglada and E. Jiménez-Piqué, Int. J.
- 18 Refract. Met. H. **23** 375 (2005)
- 19 [14] G. de Portu, L. Micele and G. Pezzotti, Acta Mater. **53** 1511 (2005)
- 20 [15] S. Suresh and E. Giannakopoulos, Acta Mater. **46** 5755 (1998)
- 21 [16] T.Y. Tsui, W.C. Oliver and G.M. Pharr, J. Mater. Res. **11** 752 (1996)
- 22 [17] Z.-H. Xu and X. Li, Acta Mater. **53** 1913 (2005)
- 23 [18] J.G. Swadener, B. Taljat and G.M.Pharr, J. Mater. Res. **16** 2091 (2001)
- 24 [19] K. Kese and D. Rowcliffe, J. Am. Ceram. Soc. **86** 811 (2003)
- 25 [20] G.M. Pharr, Mat. Sci. Eng. A. **253** 151 (1998)
- 26 [21] D.J. Morris, S.B. Myers and R.F. Cook, J. Mater. Res. **19** 165 (2004)
- 27 [22] S. Field, M.V. Swain and R.D. Dukino, J. Mater. Res. **18** 1412 (2003)
- 28 [23] F. Dahmani, J.C. Lambropoulos, A.W. Schmid, S.J. Burns and C. Pratt, J. Mat. Sci.
- 29 **33** 4677 (1998)
- 30 [24] A. Krell, and S. Schädlich, Mat. Sci. Eng. A **307** 172 (2001)
- 31 [25] J. Gong, Z. Peng and H. Miao, J. Eur. Ceram. Soc. **25** 649 (2005)
- 32 [26] C. Ullner, J. Beckmann and R. Morrell, J. Eur. Ceram. Soc. **22** 1183 (2002)
- 33 [27] P.C. Twigg, F.L. Riley and S.G. Roberts, J. Mater. Sci. **37** 845 (2002)
- 34 [28] C. Fiori and G. de Portu in *British Ceramic Proceedings 38, -Novel Ceramic*
- 35 *Fabrication Processes and Applications-* edited. by R.W. Davidge, (Shelton, Stoke-on-
- 36 Trent, (U.K.),1986)
- 37 [29] G. de Portu, L. Micele and G. Pezzotti, App. Spect. **59** 537 (2005)
- 38 [30] W.C. Oliver and G.M. Pharr, J. Mater. Res. **7** 1564 (1992)
- 39 [31] W.C. Oliver and G.M. Pharr, J. Mater. Res. **19** 3 (2004)
- 40 [32] J.C. Hay, A. Bolshakov and G.M. Pharr, J. Mater. Res. **14** 2296 (1999)
- 41 [33] A.C. Fischer-Cripps, Vacuum **58** 569 (2000)
- 42 [34] B.R. Lawn, J. Am. Ceram. Soc. **81** 1977 (1998)
- 43 [35] M. Mata and J. Alcalá, J. Mech. Phys. Sol. **52** 145 (2004)
- 44 [36] V. Sergo, D.M. Lipkin, G. de Portu and D. R. Clarke, J. Am. Ceram. Soc. **80** 1633
- 45 (1997)
- 46
- 47
- 48
- 49
- 50
- 51
- 52
- 53
- 54
- 55
- 56
- 57
- 58
- 59
- 60

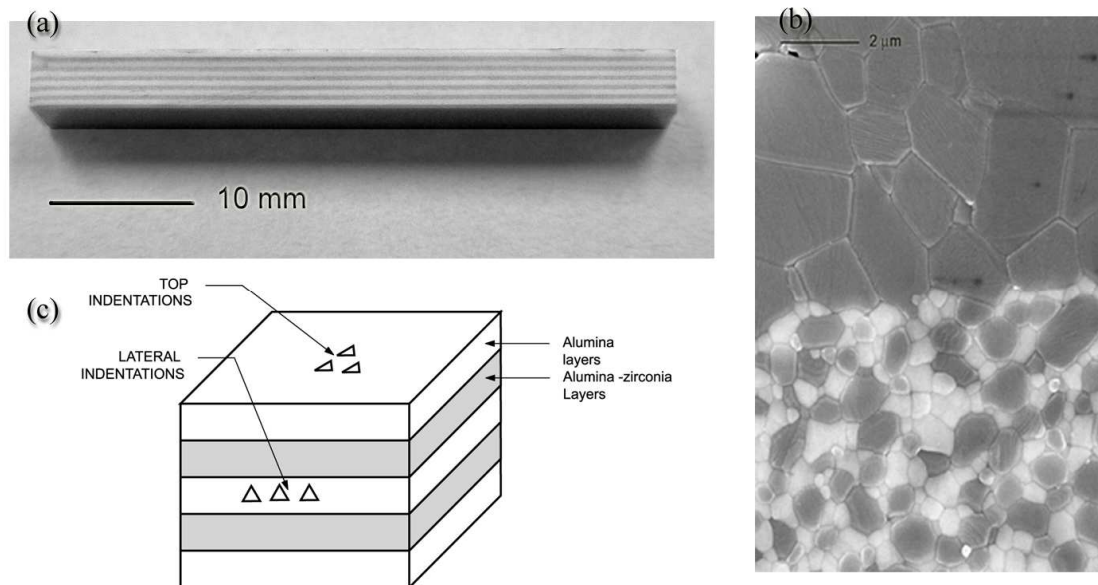


Figure 1.- a) typical A/AZ sample, where the layered architecture can be easily appreciated b) Detail of the alumina – alumina/zirconia interface c) Scheme of the indentation places

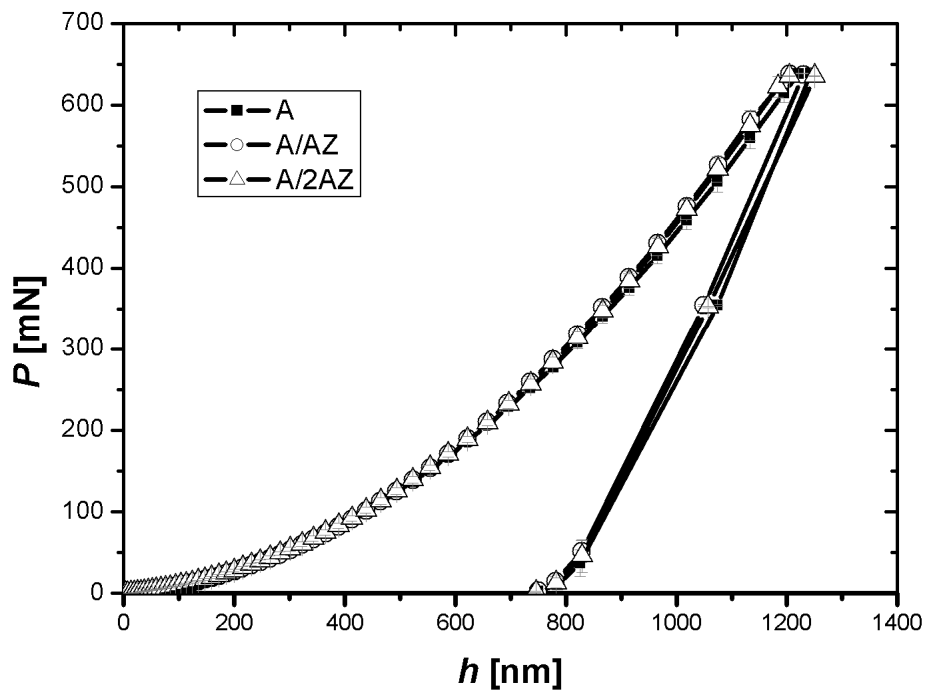


Figure 2.- P-h curve of monolithic alumina and layered materials A/AZ and A/2AZ. Average of nine indentations

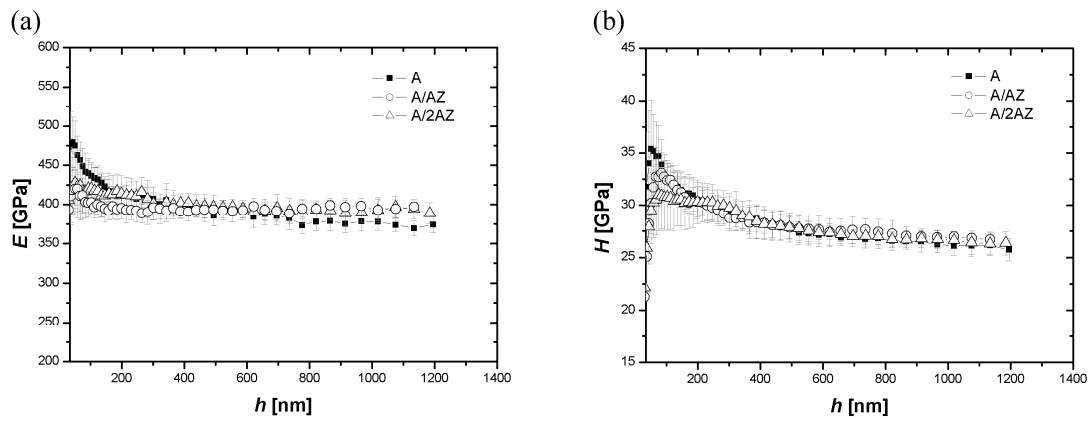


Figure 3 .- Dependence of Young's modulus (a) and hardness (b) with penetration depth of all three materials indented with Berkovich indenter.

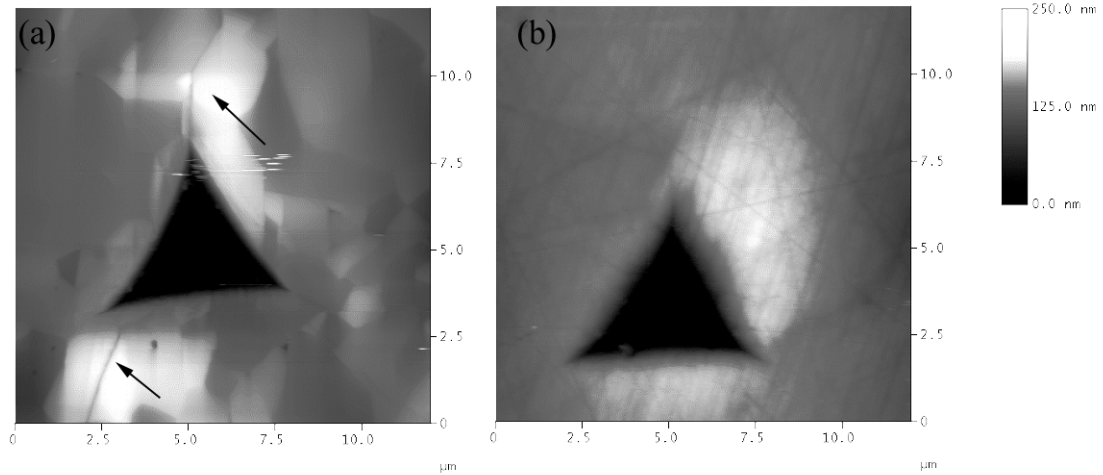


Figure 4.- AFM of the indentations imprints produced with a Berkovich indenter in alumina (a) and A/AZ laminated composite (b) with a total penetration depth of $1\mu\text{m}$. Arrows in the alumina image point the existence of radial cracks.

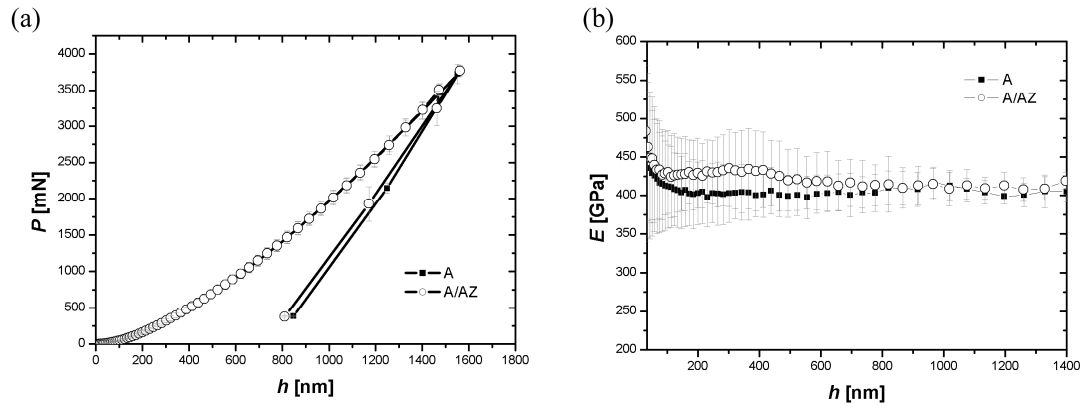


Figure 5.- Load on sample curve (a) and Young's modulus (b) vs. penetration depth with spherical indentation for alumina and A/AZ laminated composite.

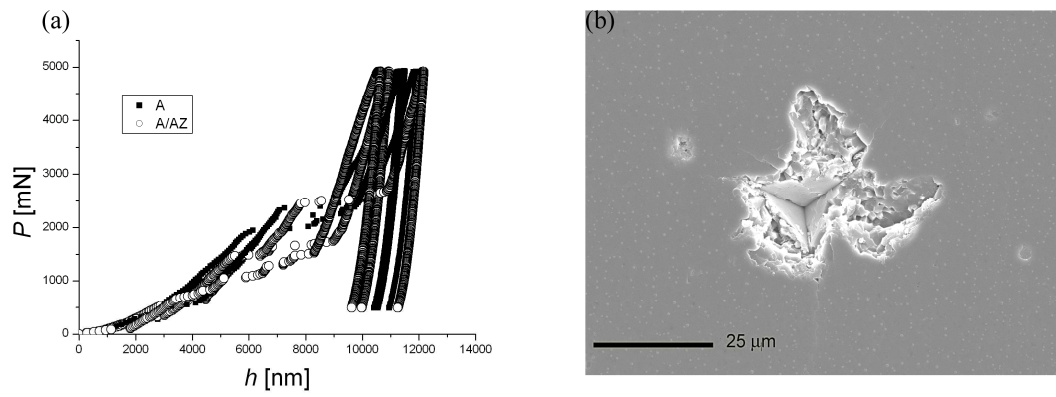


Figure 6.- Typical P-h curves obtained with cube corner indenters (a). An extensive amount of chipping was observed around all indentation imprints for every load tested.

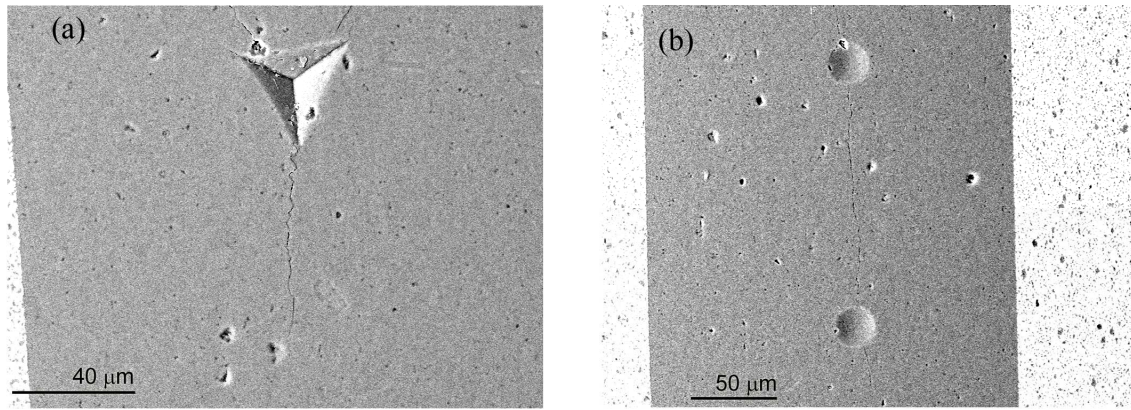


Figure 7.- Backscatter SEM pictures of Berkovich (a) and spherical indentations (b) on lateral sides of A/AZ samples. Edge stresses in lateral sides are tensile in the direction perpendicular to the interface, which results in easier propagation of radial cracking. The lack of symmetry of the stresses is clearly observable.